Diode-pumped passively Q-switched and mode-locked Nd:YLF laser with Cr^{4+}:YAG saturable absorber

Shudi Pan (潘淑娣), Kezhen Han (韩克祯), Hongmei Wang (王红梅), Xiuwei Fan (范秀伟), and Jingliang He (何京良)

College of Physics and Electronics, Shandong Normal University, Ji'nan 250014

Received January 11, 2006

A diode-pumped passively Q-switched Nd:YLF laser was demonstrated by using saturable absorber of Cr^{4+}:YAG. At the incident power of 7.74 W, pure passively Q-switched laser with per pulse energy of 210 μJ and pulse width of 19.6 ns at repetition rate of 1.78 kHz was obtained by using Cr^{4+}:YAG with initial transmission of 80%. At the incident power of 8.70 W, a Q-switched mode-locking with average output power of 650 mW was achieved, the overall slop efficiency was 16%, corresponding to the initial transmission of 85% of Cr^{4+}:YAG.

OCIS codes: 140.3530, 140.3480, 140.3540, 140.3580, 140.4050.

Compact diode-pumped passively Q-switched solid-state lasers with nanosecond pulse width and good beam quality are essential for a variety of fundamental and industrial applications. Neodymium ion-hosted crystals have been widely used to construct passively Q-switched solid-state lasers in the near-infrared region[1−6]. Each of the neodymium-doped material offers different capabilities, depending on its optical and thermo-mechanical properties. Compared with Nd:YAG and Nd:YVO_4 crystals, neodymium-doped yttrium lithium fluoride (Nd:YLF) exhibits good thermo-optical properties, which leads to stability even at large pump power. The advantage of this crystal is due to its natural birefringence and weak thermal lensing, especially to c-cut crystal corresponding to the σ polarization operating at 1053 nm. According to Ref. [7], the thermal lens effect of Nd:YLF is about a factor of 17 smaller than that of Nd:YAG under comparable pumping conditions. However the power scaling of Nd:YLF laser is hindered by the crystal's rather low stress fracture limitation, which is ~ 5 times lower than that of Nd:YAG[8]. Specifically, Nd:YLF laser transitions at 1047 and 1053 nm have upper-state lifetimes around 490 and 540 μs, respectively, versus 230 μs for Nd:YAG and around 90 μs for Nd:YVO_4, which are suited for providing higher pulse energies at kilohertz-class lasers and appropriate for pumping kilohertz-class Ti:sapphire amplifiers. The laser wavelength of 1053 nm matches the wavelength of peak gain in Nd-doped phosphate glass and usually is used as a master oscillator for Nd:glass amplifiers.

The early works on diode-pumped actively and passively Q-switched Nd:YLF lasers have been reported[8−12]. To our knowledge, continuous wave (CW) diode-pumped passively Q-switched Nd:YLF laser with Cr^{4+}:YAG as saturable absorber has not been reported in the home. In this letter, we reported a passively Q-switched c-cut 1053-nm Nd:YLF laser with Cr^{4+}:YAG saturable absorber. Pure passively Q-switching and Q-switched mode-locking laser were obtained simultaneously. In Q-switching operation, pulse energy of about 210 μJ and pulse width of 19.6 ns at repetition rate of 1.78 kHz were obtained by using Cr^{4+}:YAG with initial transmission of 80%. The Q-switched mode-locking average output power is 650 mW corresponding to the overall slope efficiency of 16% by using Cr^{4+}:YAG with initial transmission of 85%.

Cr^{4+}:YAG crystal has a saturable absorption in the range of 0.9—1.2 μm and has been widely used to generate nanosecond Q-switched and picosecond Q-switched mode-locked pulses in the near infrared region, especially in the Nd^{3+}-doped lasers operated at 1.0 μm. According to the second threshold condition, for passively Q-switched operation, the absorber saturation must occur before the gain saturation in the laser crystal. From analysis of the coupled rate equation, the criterion for good passively Q-switching is[13]

$$\frac{\ln\left(\frac{1}{T_0^2}\right)}{\ln\left(\frac{1}{T_0^2}\right)+\ln\left(\frac{1}{R}\right)+L}\frac{\sigma_{\rm gs}}{\sigma}\frac{A}{A_{\rm s}} \gg \frac{\gamma}{1-\beta},$$

where R is the reflectivity of the output mirror, σ is the stimulated emission cross section of the gain medium, L is the nonsaturable intracavity round-trip dissipative optical loss, T_0 and $\sigma_{\rm gs}$ are the initial transmission and the ground-state absorption cross section of the saturable absorber. The ratio $A/A_{\rm s}$ is the effective area in the gain medium to that in the saturable absorber, the inversion reduction factor $\gamma = 1$ or $\gamma = 2$ corresponds to four-level or three-level systems, β is the ratio of the excited-state absorption (ESA) cross section to that of the ground-state absorption in the saturable absorber. In the experiment, the following parameters were used to calculate: $\sigma_{\rm gs} = 7\times10^{-18}$ cm^2, $\beta = 0.28$[14], $L = 0.01$, $R = 0.9$, $T_0 = 0.85$ or $T_0 = 0.8$, $\gamma = 1$, $A/A_{\rm s} = 2$. When the intracavity intensity is high enough, all Cr^{4+} ions are quickly excited to the first excited state, and the strong ESA causes a great quantity of Cr^{4+} ions accumulated in higher levels, which leads to saturation of the ESA. Since the relaxation time of the ESA is in the subnanosecond region, it is possible to achieve a passively Q-switched mode-locking operation with Cr^{4+}:YAG saturable absorber if the intracavity laser intensity is large enough[4−6].

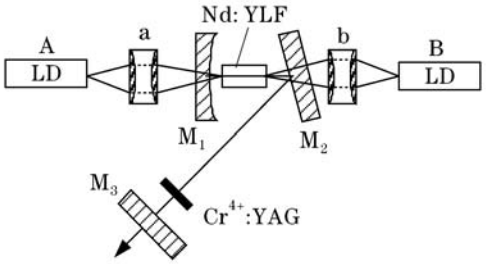

Fig. 1. Configuration of a passively Q-switched Nd:YLF laser with Cr^{4+}:YAG as saturable absorber.

The schematic of our experimental setup is shown in Fig. 1. Dual-end-pumped strategy with two diode lasers operated at different wavelengths was employed. The pump sources A and B are rated at a maximum power of 8 W around wavelength of 808 nm and 5 W around wavelength of 796 nm, respectively. Because the Nd:YLF crystal's higher absorption coefficient for pump wavelength is around 796 nm and the absorption bandwidth is narrower, the bandwidth of lower absorption coefficient around 808 nm is wider. We employed two diode lasers of different pump wavelengths instead of detuning the pump wavelength from the absorption peak[15], to increase the absorption efficiency of pump power and reduce the risk of stress fracture. Dual-end-pumped strategy can distribute the pump absorption over the length of the crystal, which can reduce the risk of stress fracture too. The diameter and numerical aperture are 0.8 mm and 0.2 for fiber bundle A, while 0.4 mm and 0.22 for fiber bundle B. The spot sizes of the pump beam on laser crystal are 0.7 and 0.6 mm by use of coupling collimators a and b. The c-cut $4 \times 4 \times 8$ (mm) Nd:YLF crystal, with 1.0% Nd^{3+} concentration, was coated for antireflection at 796 and 1053 nm on both end faces. The crystal was wrapped with indium foil and then mounted in a water-cooled copper block. The water temperature was maintained at 25 °C. The resonator consisted of three mirrors: two input mirror M_1 (R = 200 mm) and M_2 ($R = \infty$) with high transmission at 796 nm and high reflection at 1053 nm, flat mirror M_3 as the output. The length of the cavity was about 100 mm. By matrix $ABCD$, the laser mode radii were ~ 186 μm on the absorber and ~ 260 μm inside the Nd:YLF crystal. Various output mirrors with transmissions of 3.5%, 10%, 20% were tested and we found that an output coupler with transmission of 10% at 1053 nm gave the optimum performance through their average output powers in the experiment. Two 1053 nm anti-reflection coated Cr^{4+}:YAG crystals with initial transmissions of 80% and 85% were used. The Cr^{4+}:YAG saturable absorber was inserted into the laser cavity near the output mirror where the laser beam spot size was at the minimum. The Q-switched laser output beam was detected with a high speed InGaAs photo detector (New Focus 1623) and a digital oscilloscope (Tektronix TDS 5104).

The comparison of the average output power as a function of the incident pump power with different initial transmissions of Cr^{4+}:YAG was depicted in Fig. 2. The incident power from A was stabilized at 3.5 W, while the incident power from B was increased gradually in our experiment. The threshold of incident power is 4.95 W for $T_0 = 80\%$ and 4.30 W for $T_0 = 85\%$ of Cr^{4+}:YAG.

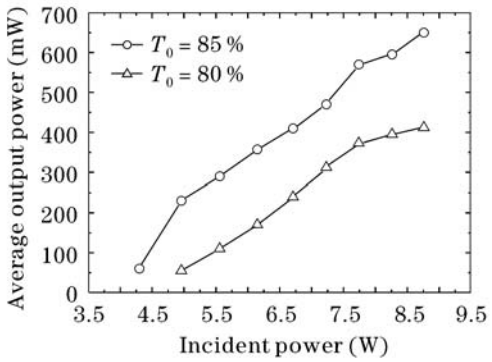

Fig. 2. Dependence of average output power on incident power with $T_0 = 85\%$ and $T_0 = 80\%$ of Cr^{4+}:YAG.

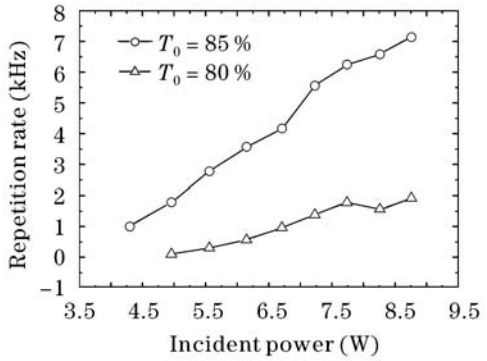

Fig. 3. Dependence of repetition rate on incident power for $T_0 = 85\%$ and $T_0 = 80\%$ of Cr^{4+}:YAG.

The laser exhibits pure Q-switching operation within the ranges of incident power from 4.30 to 6.70 W corresponding to $T_0 = 85\%$ and from 4.95 W to 7.74 W corresponding to $T_0 = 80\%$ of Cr^{4+}:YAG. The mode-locked pulses were modulated upon the Q-switched pulse envelope within the ranges of incident power from 6.70 to 8.70 W and 7.74 to 8.70 W corresponding to $T_0 = 85\%$ and $T_0 = 80\%$ of Cr^{4+}:YAG. The maximum average output powers were 650 and 412 mW at the incident power of 8.70 W, the overall slop efficiencies were 16% and 10% with the $T_0 = 85\%$ and $T_0 = 80\%$ of Cr^{4+}:YAG, respectively. Figure 3 presents the frequency repetition rate as a function of incident power using Cr^{4+}:YAG with different initial transmissions. During the range of incident power from laser threshold to maximum, the repetition rate increased from 0.1 to 1.92 kHz for $T_0 = 80\%$, while from 1.79 to 7.14 kHz for $T_0 = 85\%$ of the saturable absorber. The threshold of incident power was higher, average output power and repetition rate by use of $T_0 = 80\%$ were lower than those by use of $T_0 = 85\%$ of Cr^{4+}:YAG. Because the saturable absorber of lower initial transmission has a larger density of Cr^{4+} that leads to a larger intracavity loss, and accordingly, the higher the threshold was, the lower the average output power and repetition rate were achieved. At the incident power of 7.74 W, the Q-switched pulse width was 19.6 ns (as shown in Fig. 4) and the repetition rate was 1.78 kHz, corresponding to the pulse energy of 210 μJ with $T_0 = 80\%$, while 29.7 ns, 6.25 kHz, and 86 μJ with $T_0 = 85\%$ of the saturable absorber. Figure 5 presents the temporal shapes of Q-switched mode-locked pulses with different initial transmissions of Cr^{4+}:YAG at the

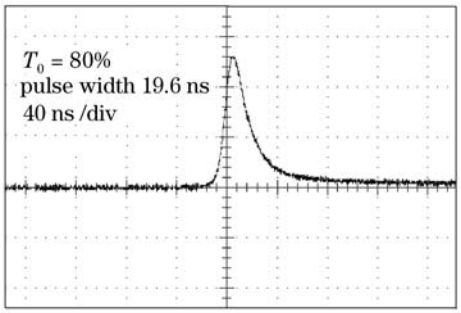

Fig. 4. Temporal trace of a single Q-switched pulse for T_0 = 80% of Cr^{4+}:YAG at incident power of 7.74 W.

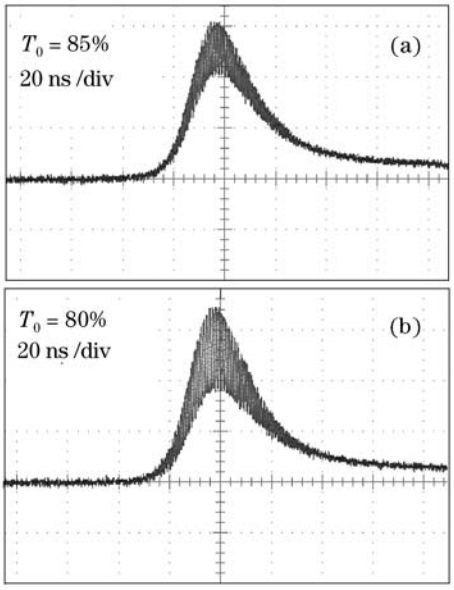

Fig. 5. Temporal shapes of single Q-switched mode-locked pulse for T_0 = 85% (a) and T_0 = 80% (b) of Cr^{4+}:YAG.

same incident power of 8.70 W. The modulation depth enhanced and the full-width at the half-maximum (FWHM) of the Q-switched pulse envelope varied little as the incident power was increased. We did not measure the width of the envelope because of the instability of the Q-switched mode-locked pulses. It is obvious that the modulation depth is about 45% for T_0 = 80% and just about 20% for T_0 = 85% of the saturable absorber. The phenomena can be explained that Cr^{4+}:YAG crystal with lower initial transmission needs a higher energy to saturate the ESA. As a result, Q-switched mode-locked pulse with higher modulation depth was achieved by use of lower initial transmission of Cr^{4+}:YAG. It is obvious that Q-switched mode-locking with 100% modulation depth can be obtained if higher incident power and lower initial transmission of Cr^{4+}:YAG are available.

In conclusion, we have demonstrated a passively Q-switched mode-locked Nd:YLF solid-state laser with different initial transmissions of Cr^{4+}:YAG. At the incident power of 7.74 W, pure passively Q-switched laser with per pulse energy of 210 μJ and the pulse width of 19.6 ns at repetition rate of 1.78 kHz was obtained by use of T_0 = 80% of Cr^{4+}:YAG. We believe that this laser is feasible in applications of master oscillator power amplifier (MOPA) of Nd:glass. At the incident power of 8.70 W, a Q-switched mode-locking with average output power of 650 mW was achieved with the overall slop efficiency of 16%, corresponding to T_0 = 85% of Cr^{4+}:YAG. At the maximum incident power, the modulation depth is about 45% for T_0 = 80% and just about 20% for T_0 = 85% of the saturable absorber.

This work was supported by the National Natural Science Foundation of China under Grant No. 60478009. J. He is the author to whom the correspondence should be address, his e-mail address is hejl@sdnu.edu.cn.

References

1. J. Wang, W. Zhang, Q. Xing, and Q. Wang, Opt. Laser Technol. **30,** 303 (1998).
2. C. Du, J. Liu, Z. Wang, G. Xu, X. Xu, K. Fu, X. Meng, and Z. Shao, Opt. Laser Technol. **34,** 699 (2002).
3. Y. F. Chen, S. W. Chen, Y. C. Chen, Y. P. Lan, and S. W. Tsai, Appl. Phys. B **77,** 493 (2003).
4. T. M. Jeong, C.-M. Chung, H. S. Kim, C. H. Nam, and C.-J. Kim, Electron. Lett. **36,** 633 (2000).
5. Y.-F. Chen and S. W. Tsai, IEEE J. Quantum Electron. **37,** 580 (2001).
6. Y.-F. Chen, J.-L. Lee, H.-D. Hsich, and S.-W. Tsai, IEEE J. Quantum Electron. **38,** 312 (2002).
7. C. Pfistner, R. Weber, H. P. Weber, S. Merazzi, and R. Gruber, IEEE J. Quantum Electron. **30,** 1605 (1994).
8. W. A. Clarkson, P. J. Hardman, and D. C. Hanna, Opt. Lett. **23,** 1363 (1998).
9. H. Zhang, K. Du, D. Li, P. Shi, Y. Wang, and R. Diart, Appl. Opt. **43,** 2940 (2004).
10. B. Frei and J. E. Balmer, Appl. Opt. **33,** 6942 (1994).
11. H. Plaessmann, F. Stohr, and W. M. Grossman, IEEE Photon. Technol. Lett. **3,** 885 (1991).
12. X. Peng, L. Xu, and A. Asundi, Appl. Opt. **44,** 800 (2005).
13. G. Xiao and M. Bass, IEEE J. Quantum Electron. **33,** 41 (1997).
14. Z. Burshtein, P. Blau, Y. Kalisky, Y. Shimony, and M. R. Kokta, IEEE J. Quantum Electron. **34,** 292 (1998).
15. E. C. Honea, R. J. Beach, S. B. Sutton, J. A. Speth, S. C. Mitchell, J. A. Skidmore, M. A. Emanuel, and S. A. Payne, IEEE J. Quantum Electron. **33,** 1592 (1997).